An energy-saving model based predictive control strategy for thermoelectric water cooler dispenser

Daniel Lopes Amaral, Bismark Claure Torrico, Marcos Uchoa Cavalcante
Universidade Federal do Ceará, Department of Electrical Engineering
Mister Hull Avenue, Postal code: 60455-760, Fortaleza, Ceará, Brazil
Email: daniel.amaral@dee.ufc.br, bismark@dee.ufc.br, uchoacavalcante@dee.ufc.br

***Abstract*—A Model Based Predictive Control was applied to temperature control of a thermoelectric fluid cooling system in order to attain performance requirements considering equipment operational limits and standard brochure. A phenomenological linear model was obtained and its parameters were identified by least squares algorithm. Simulation and experiments showed satisfactory compromise by simulation capability and residue characteristic criterion. The closed loop system behavior allowed energy saving in standby temperature regulating compared to electronic thermostat and achieved ENERGYSTAR energy-efficiency criteria certification requirements infeasible for traditional regulation.**

I. Introduction

The thermoelectric cooling technology has been widely used in small refrigerators, beer chillers and wine cellars [1]. However, many commercial water cooler models still employ heat pumping compression principle based on motor compressors, condensers, expansion devices, evaporators and electromechanical thermostats like US2912142 [2] first dispenser patent. Moreover, the compression circuit replacement for thermoelectric modules provides benefits like absence of moving parts and noise, reduced size and weight, high reliability and repeatability, and low power consumption that makes the thermoelectric technology an alternative to traditional motor compressors [3].

Feedback control systems emerge as solution to thermoelectric water coolers temperature regulation problem: the inner temperature dynamic modeling and system identification are tools for controller tuning based on process model [4]. More sophisticated controllers design may accomplish the temperature regulating with energy saving, economic components design and unfeasible specifications for bistable control based on inherited compression principle [5].

Therefore, this research original technical result is the thermostat temperature based regulation replacement for a model based predictive control design such that the new strategy allows the system achieving specified requirements in ASHRAE/ANSI18: Methods of Testing for Rating Water Coolers with Self-Contained Mechanical Refrigeration [6] and attending ENERGYSTAR [7] energy-efficiency criteria.

This paper has been organized as follow: in section 2 the thermoelectric cooler system has been approached; in section 3 the dynamic model has been modeled; in section 4 the model parameter identification experiment is characterized; in section 5 the model based predictive control is designed; in section 6 the results are presented; the conclusions are made in section 7, followed by references.

II. Thermoelectric Cooler Characterization

The experimental bench Fig. 1 allows cooling performance analysis by inner reservoir water temperature, room temperature, electric current and thermoelectric module voltage.

Fig. 1. Experimental bench.

The refrigeration system comprises the thermoelectric cooler, data acquisition, processing and control, communication module and power drive as Fig. 2:

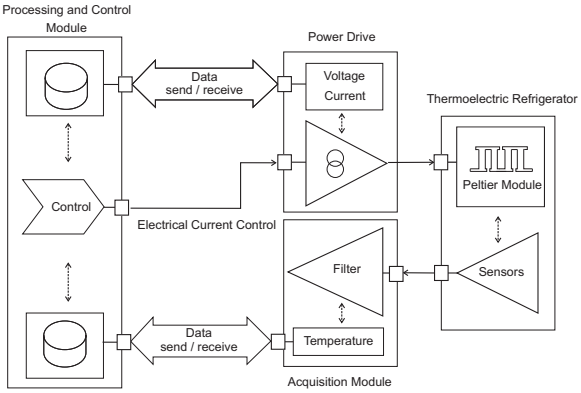

Fig. 2. Modules integration.

The thermoelectric cooler is permanently water occupied reservoir surrounded by polyurethane foam. Internal heat sink fins are in thermal contact with the fluid and its base is linked on Peltier module cold face. External heat sink base is on module hot face and its fins are in room air thermal contact.

III. Dynamic Model

The process dynamic behavior is governed by thermal and electrical agents interaction. The electric current determines the thermal power pumped by the module, while the material properties and thermodynamic design defines the temperature in each region [8]. Model description considers the fluid, the module faces and thermoelements energy balance. Boundary conditions, approximations and linearization are defined and temperature is carried out at concentrated parameters [9].

A. Thermodynamic System Modeling

The model dynamics equations consider heat flow through masses coupled to module and thermoelements mass. The thermal load Q_L is the heat pumped by the thermoelectric module. Eq. (1) models thermoelements energy balance:

$$Q_L - Q_k - I\alpha_{pn}T_L = (m_l c_l + m_c c_c)\frac{dT_L}{dt} \quad (1)$$

$$Q_k = -kA\left.\frac{\partial T(x,t)}{\partial x}\right|_{x=0}$$

where Q_k is the cold face conduction heat absorbed; $I\alpha_{pn}T_L$ is the absorbed Seebeck effect energy; $T(x,t)$ is the one-dimensional temperature distribution function in thermoelements; k is the thermoelectric material thermal conductivity; A is the thermoelements cross sectional sum area; m_l is the internal heat exchanger mass; c_l is the internal heat exchanger specific heat; m_c is the thermoelements mass and c_c is the thermoelements specific heat. Eq. (2) models external heat exchange energy flow:

$$I\alpha_{pn}T_H + Q_o - Q_c = (m_f c_f + m_H c_H)\frac{dT_H}{dt} \quad (2)$$

$$Q_c{=}hA_F(T_H - T_{amb}); Q_o{=}{-}kA\left.\frac{\partial T(x,t)}{\partial x}\right|_{x=L}$$

where Q_o is the thermal energy conducted to thermoelements hot surface; Q_c is the convection heat transmitted from external heat sink to room; $I\alpha_{pn}T_H$ is Seebeck effect hot face dissipated energy; T_{amb} is room temperature; h sink convection coefficient; A_F convection effective area; m_f external heat exchanger mass; c_f external heat exchanger specific heat; m_H thermoelements mass and c_H thermoelements specific heat. The Fourier Equation (3) describes thermoelements energy flow:

$$k\frac{\partial^2 T(x,t)}{\partial x^2} - \frac{\tau}{A}I\frac{\partial T(x,t)}{\partial x} + \frac{\rho}{A^2}I^2 = AC\gamma\frac{\partial T(x,t)}{\partial t} \quad (3)$$

where the boundary conditions are given by $T(0,t) = T_L(t)$ and $T(L,t) = T_H(t)$. Eq.(3) describes Peltier, Thomson and Joule effects, where τ is the Thomson coefficient; ρ electrical resistivity average; C is the thermoelements specific heat and γ is the thermoelements specific mass.

B. Model Linearization

Model Linearization is based on small signals analysis. The magnitudes are presented as steady state value added to a perturbation around it *e.g.* $I(t) = \bar{I} + \tilde{I}(t)$ for electric current. It is performed due materials properties temperature dependence. Transfer function considers only perturbed signals.

C. Process Transfer Function

The transfer functions from $\tilde{Q}_L(s)$, $\tilde{T}_{amb}(s)$ and $\tilde{I}(s)$ to $\tilde{T}_L(s)$ leads second order systems with different zeros and gains for each input variable. Since $\tilde{Q}_L(s)$ is the heat flow to module cold face in a generic way, it is modified to represent the cooling fluid energy flow.

The heat pump draws energy from fluid via internal heat sink by convection, such that the energy flow entering in the system is associated with convection from ambient to water through the insulator and sensitive heat necessary to water temperature change. Water mass was added to system leading a third order system related to the thermal capacity of the two heat sinks and the cooled fluid.

In addition the room temperature variation are strongly attenuated by the thermal insulator ($\tilde{T}_a(s) = 0$), ie, considered as model disturbance.

IV. Model Parameter Identification

System identification techniques are used to provide a parameterized model that simulates the fluid temperature behavior by applying direct current on specified linear operation region [10]. The water reservoir temperature $\tilde{T}_f(t)$ can be described by discrete transfer function Eq.(4) with sampling period T_s; $a_j = a_j(\bar{I}_o)$ and $b_k = b_k(\bar{I}_o)$ are model parameters as $\bar{I}_o$ function. The excitation current is $\tilde{I}_o$ and $e(t)$ represents unmodeled dynamics:

$$\tilde{T}_f(t) = -\sum_{j=1}^{m} a_j\tilde{T}_f(t - jT_s) + \sum_{k=1}^{n} b_k\tilde{I}_o(t - kT_s) + e(t) \quad (4)$$

Identification experiment is carried out disturbing system current $\tilde{I}_o = \pm 0.75A$ around the bias current $\bar{I}_0 = 1.00A$, which corresponds to ANSI18 maximum water temperature on controlled room temperature ($\bar{T}_{amb} = 27.50 \pm 0.25^o$C).

A. Model Structure and Prediction Error

Eq. (5) describes a linear model structure for one step ahead predictor:

$$\tilde{T}_f(t|t-1, \theta(\bar{I}_o)) = \phi(t-1)^T\theta(\bar{I}_o) \quad (5)$$

where $\phi(t-1) = [-\tilde{T}_f(t-1) \quad \dots \quad -\tilde{T}_f(t-m) \quad \tilde{I}_o(t-1)\dots\tilde{I}_o(t-n)]$)] is the regressors vector and $\theta(\bar{I}_o) = [a_1 \dots a_m \quad b_1 \dots b_n]$] is the parameters vector associated to $\bar{I}_o$ and have its order limited to $m+n$ based on phenomenological model order. Parameter vector $\theta(\bar{I}_o)$ is determined by

one step ahead prediction error cost function J_i as Eq. (6):

$$J_i = \sum_{t=1}^{N} \left[T_{exp}(t) - \tilde{T}_f(t|t-1, \theta(\bar{I}_o)) \right]^2 \quad (6)$$

minimization according to Eq. (7):

$$\theta(\bar{I}_o) = \arg \min_{\theta(\bar{I}_o) \in \mathcal{D}} J_i \quad (7)$$

where $T_{exp}(t)$ is the experimental value, N is total experiment samples and $\mathcal{D}$ limits the parameter vector search space to $m+n$.

B. Identification Experiment Design

The identification experiment consists in applying a six order pseudo-randon binary sequence (PRBS) current signal added to bias current selected based on discrete model order limit [10].

Additional PRBS characteristics are defined through system step response as Fig. 3:

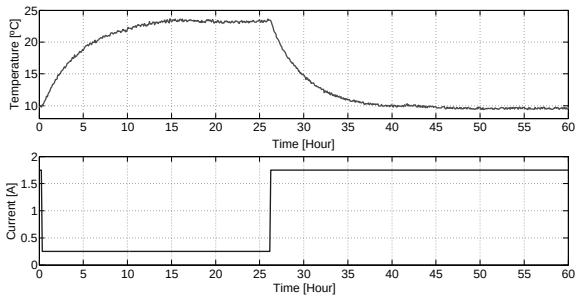

Fig. 3. Electrical current step response.

Approaching system by first order equivalent, its time constant is 4.20h and reaches steady state after 20h. Considering interval between samples $T_b = 25$min and excitation signal period $T_{i(t)} = 26.25$h. Three excitation signal periods response are shown as Fig. 4:

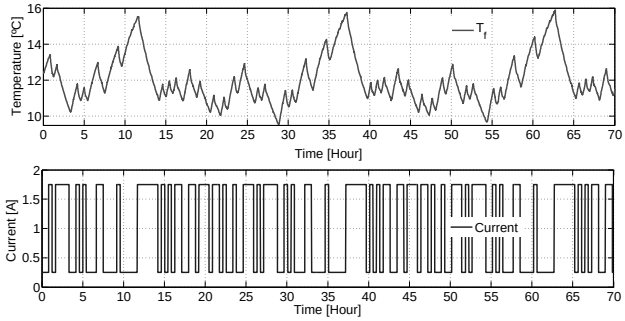

Fig. 4. PRBS reponse.

C. Parameter Identification

The first half experimental data was used for identification purpose, while the second half is used for model validation. The search space is investigated due the non direct equivalence between zeros in continuous and discrete models [11], where $1 \leq m, n \leq 3$ and $m \leq n$ describes a proper system.

The Final Prediction Error Akaike - *FPE* function was used for indexes the relationship between model order and the residue variance. Lower value corresponds to the most appropriate model based on the error correlation to explain the experimental data by simulation. It envolves the loss function V, the number of estimated parameters $d = m + n$ and the number of available samples for validation N:

$$FPE = V\left(\frac{1+d/N}{1-d/N}\right); V = det\left(\frac{1}{N}\sum_{k=1}^{N} \varepsilon(k,\hat{\theta})\varepsilon(k,\hat{\theta})^T\right)$$

considering $d \ll N$ them $FPE = V(1+d/N)$, where $\varepsilon(k,\hat{\theta})$ is the simulation error committed for k-th sample.

Apart from *FPE*, it is used the *FIT* index which calcules the output experimental data ratio explained by model simulation:

$$FIT = 1 - \sqrt{\frac{\sum_{k=1}^{N}[\tilde{T}_f(k) - T_{exp}(k)]^2}{\sum_{k=1}^{N}[T_{exp}(k) - \bar{T}_{exp}]^2}}$$

The model that maximizes *FIT* and minimizes *FPE* is adopted as the best one to represent the process: the criterion relates compromise between simulation capability and residue correlation properties. The process can be modeled by a first order discrete transfer function with $T_s = 300s$:

$$\tilde{H}(z, \bar{I}_o = 1.00A) = -\frac{0.179z^{-1}}{1 - 0.9772z^{-1}} \quad (8)$$

The residual analysis is used to check the experimental value characteristics not explained by the simulation shown in Fig. 5:

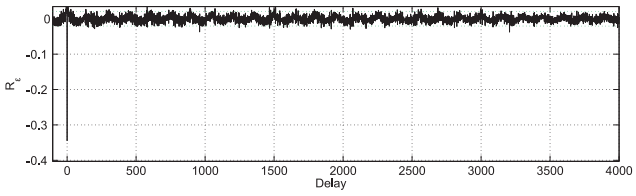

Fig. 5. Whiteness Test: $\tilde{H}^{-1}(z, \bar{I}_o)$ filtered residue autocorrelation.

The residue correlation uniformity allows affirming that it is a white noise, as assumed in Eq 4, while the periodicity is due to dynamic room temperature bistable control not explained by $\tilde{H}(z, \bar{I}_o = 1.00A)$ as Fig 6:

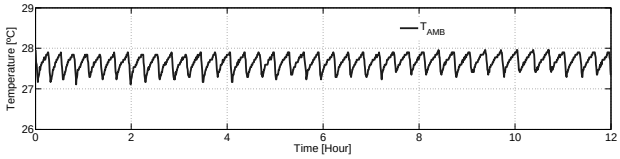

Fig. 6. Bistable room Temperature Control.

Models are listed on table I:

A second experiment was carried out in order to assess model simulation capacity as shown in Fig 7. The PRBS signal was realized with order $b = 8$ and $T_b = 7$ minutes, where

TABLE I
ORDER, INDEXES AND REGRESSORS

mn	*FIT*	*FPE*	φ
1 1	86.47	3.07	[-0.9772 -0.1790]
2 1	85.66	3.47	[-1.3260 0.3409 -0.1290]
2 2	86,09	3.26	[0.0365 -0.9833 -0.2745 -0.2903]
3 1	85.46	3.56	[-1.0280 -0.0987 0.1444 -0.1561]
3 2	85.93	3.34	[-0.2891 -0.8557 0.1777 -0.1094 -0.1837]
3 3	86.30	3.16	[0.0246 -0.2618 -0.7035 -0.0780 -0.2283 -0.2226]

$T_{i(t)} = 29.75$h and has enlarged spectral band: T_{exp} is the fluid temperature and T_{sim} is the simulated temperature.

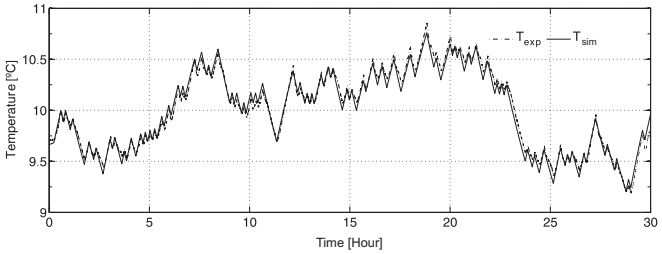

Fig. 7. PRBS test: *FIT* = 85.72 and *FPE* = 4.44.

V. MODEL BASED PREDICTIVE CONTROL DESIGN

The model based predictive control - MBPC system structure adopted is shown in Figure 8. MBPC strategies uses explicit model to predict the plant outputs and calculate future inputs by cost function optimizing that considers the control objectives, reference trajectory and constraints [12].

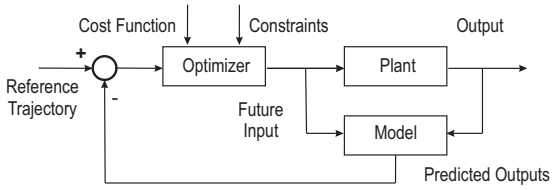

Fig. 8. MBPC structure.

The cost function $J(N_1, N_2, N_u, \lambda)$ is given by:

$$J=\sum_{k=N_1}^{N_2}[w(t+k) - \hat{y}(t+k|t)]^2 + \lambda\sum_{k=1}^{N_u}[\triangle u(t+k-1)]^2 \quad (9)$$

where $\hat{y}(t+k|t)$ is the k steps ahead output prediction based on given t instant information, $\triangle u$ is the control signal variation, $\triangle = 1 - z^{-1}$ is the difference operator, w is the future trajectory reference, λ is the weighting control effort, N_u is the control horizon, N_1 and N_2 define the prediction horizon. The plant is described by Controlled Auto-Regressive Integrated Moving Average model:

$$A(z^{-1})y(t) = z^{-d}B(z^{-1})u(k-1) + \frac{1}{\triangle}\varepsilon(t) \quad (10)$$

where $\varepsilon(t)$ is white noise. The future outputs are accomplished by *Diophantine equation*:

$$1 = E_k(z^{-1})\triangle A(z^{-1}) + z^{-k}F_k(z^{-1}) \quad (11)$$

applied to plant model:

$$y(t+k) = F_k y(t) + E_k B(z^{-1})\triangle u(t+k-1) + E_k\varepsilon(t+k) \quad (12)$$

omitting the argument (z^{-1}). Since $\mathbf{E}[\varepsilon(k)] = 0$ and $\mathbf{E}[\varepsilon(k)\varepsilon(j)] = 0, \forall k \neq j$, where $\mathbf{E}[.]$ is expectation operator:

$$E_k(z^{-1})B(z^{-1}) = G_k(z^{-1}) + z^{-k}G'_k(z^{-1}) \quad (13)$$

optimum plant output prediction is given by:

$$\hat{y}(t+k|t) = G_k\triangle u(t+k-1) + F_k y(t) + G'_k\triangle u(t-1) \quad (14)$$

writing J in matrix notation:

$$\underbrace{\begin{bmatrix}\hat{y}(t+N_1|t)\\ \hat{y}(t+N_1+1|t)\\ \vdots \\ \hat{y}(t+N_2|t)\end{bmatrix}}_{\hat{Y}} = \underbrace{\begin{bmatrix}G_{N_1}\\ G_{N_1+1}\\ \vdots \\ G_{N_2}\end{bmatrix}}_{G}\triangle\mathbf{u} + \underbrace{\begin{bmatrix}F_{N_1}\\ F_{N_1+1}\\ \vdots \\ F_{N_2}\end{bmatrix}y(t) + \begin{bmatrix}G'_{N_1}\\ G'_{N_1+1}\\ \vdots \\ G'_{N_2}\end{bmatrix}u(t-1)}_{f}$$

where $\triangle\mathbf{u}$ corresponds to the stacking $\triangle\mathbf{u} = [\triangle u(t)\, \triangle u(t+1) \ldots \triangle u(t+N_u-1)]^T$. For reference trajectory $\mathbf{W} = [w(t+N_1)\, w(t+N_1+1)\, \ldots\, w(t+N_2)]^T$ and G_{N_1+i} are polynomials:

$$\begin{aligned} J &= (\mathbf{W}-\hat{Y})^T(\mathbf{W}-\hat{Y}) + \triangle\mathbf{u}^T\lambda\triangle\mathbf{u} \\ &= \frac{1}{2}\triangle\mathbf{u}^T H\triangle\mathbf{u} + b^T\triangle\mathbf{u} + f_0 \end{aligned}$$

where,

$$H = 2(GG^T+\lambda I); \quad b^T = 2(f-\mathbf{W})^T G; \quad f_0 = (f-\mathbf{W})^T(f-\mathbf{W})$$

for each discretization period a Quadratic Programming Problem is written:

$$\triangle\mathbf{u}: \quad \begin{matrix}\text{minimize} & \frac{1}{2}\triangle\mathbf{u}^T H\triangle\mathbf{u} + b^T\triangle\mathbf{u} + f_0 \\ \text{subject to} & R\triangle\mathbf{u} \leq l\end{matrix}$$

for only control signal amplitude restrictions:

$$R = \begin{bmatrix} T \\ -T \end{bmatrix} \quad e \quad l = \begin{bmatrix} I(u_{max} - u(t-1)) \\ I(u(k-1) - u_{min}) \end{bmatrix}$$

where T is a lower triangular matrix, I is an identity matrix, u_{max} and u_{min} are the upper and lower control signal limits [13].

Due receding control strategy is applied to process only first element of $\triangle\mathbf{u}$:

$$u(t) = \triangle u(t) + u(t-1)$$

ie, once obtained the control sequence $\triangle\mathbf{u}$, is calculated the input signal to be applied to plant based only on $\triangle u(t)$, it is updating output and input signal information and solves optimization problem again. For all experiments presented, only the first order parameterized model is used for output plant predictions and control tuning is fixed as $N_1 = 1$, $N_2 = 50$, $N_u = 48$, $u_{max} = 3$, $u_{min} = 0$ and $\lambda = 45$ as [14].

Fig. 9 presents fluid temperature T_f dynamic behavior as reference tracking and regulation on not controlled room temperature T_{amb} at closed loop operation within the linear region.

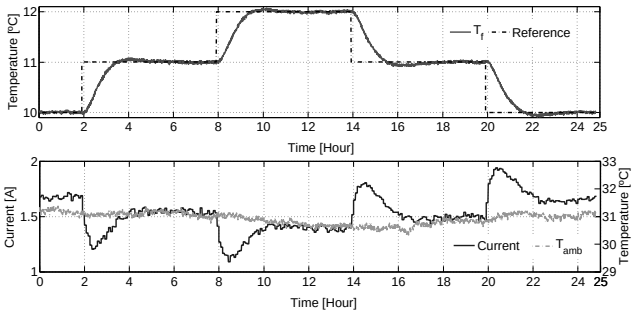

Fig. 9. MBPC: linear region.

The experiment illustrated in Fig. 10 exposes the reference tracking and regulation, expanding temperature excursion outside linear limits and determines the minimum temperature reached by saturating control signal.

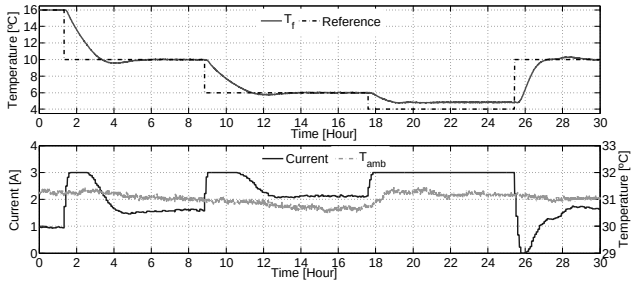

Fig. 10. MBPC: saturating control sinal.

The water density anomalous behavior is shown in Figure 11. In this case, the water density has non-linear behavior around 4^oC [15] generating convection currents differing in the control volume, which represents an economic limit to the practical system. Additionally, the experiment characterizes the ability to regulate at 6^oC from the nonlinear region.

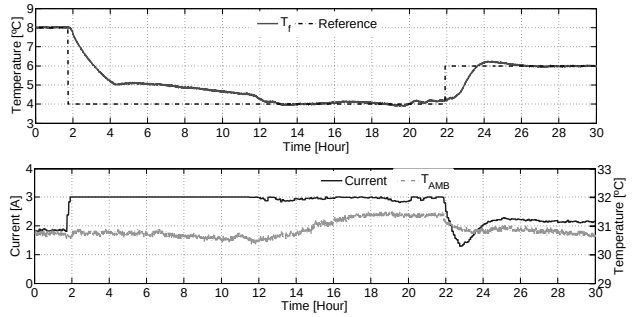

Fig. 11. MBPC: strong non linearity.

Fig. 12 presents MBPC regulation mode performance when the system is disturbed by draining 180ml of reservoir water and Fig. 13 presents results for the same experiment for bistable control. After 12h, four 180ml portions each every 15min were drained with volume replacement at room temperature. The experiment is carried out in order to evaluate the system cooling capacity according to normative criteria [6].

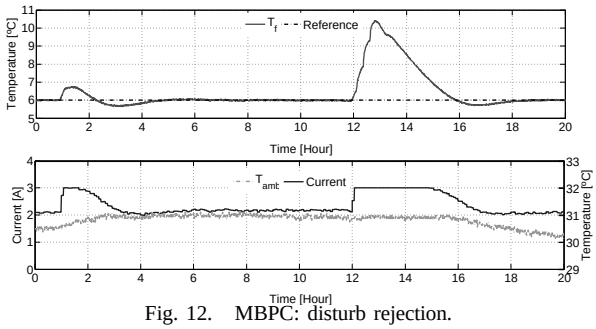

Fig. 12. MBPC: disturb rejection.

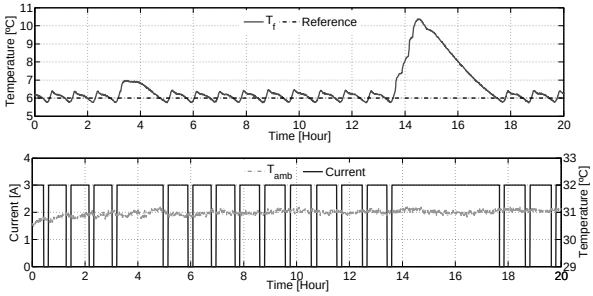

Fig. 13. Thermostat: Disturb Rejection.

As soon as disturbance was detected, the control signal comes into saturation, with the benefit of ensuring fewer oscillations, lower overshot and the same peak temperature as bistable control. Comparing experiments results shown in Figs. 12 and 13, the time for disturbances rejection and cooling capacity are equivalent for both methods.

VI. Results

The experiments reported in Figs. 14 and 15 are performed in order to evaluate the power consumption over 24h period for ENERGYSTAR certificate criteria set-point temperature regulation [7] as table II:

TABLE II
ENERGYSTAR Energy-Efficiency Criteria.

Water Cooler Category	Standby Energy Consumption [KWh/day]
cold only unit	≤ 0.16
hot and cold unit	≤ 1.20

Adapted from [7].

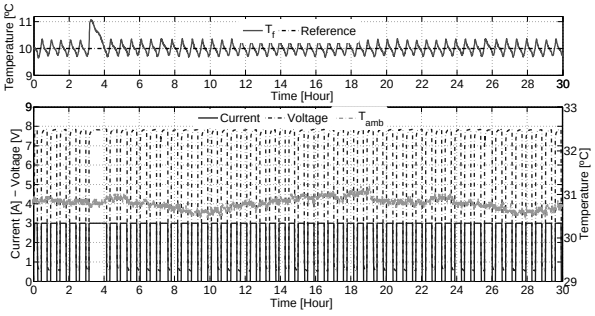

Fig. 14. Electrical energy consumption at 10^oC: thermostat.

Table III presents the results related to the experiments reported in Figs. 14, 15, 16 and 17 to calculate standby energy consumption.

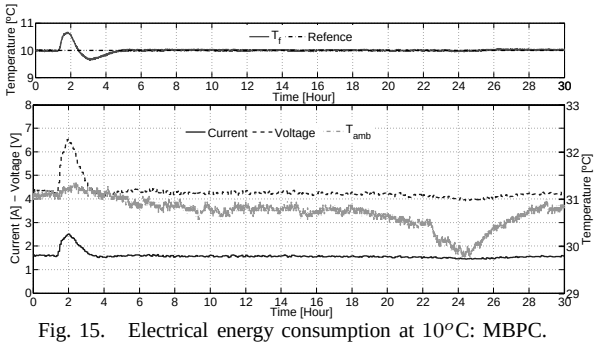

Fig. 15. Electrical energy consumption at 10^oC: MBPC.

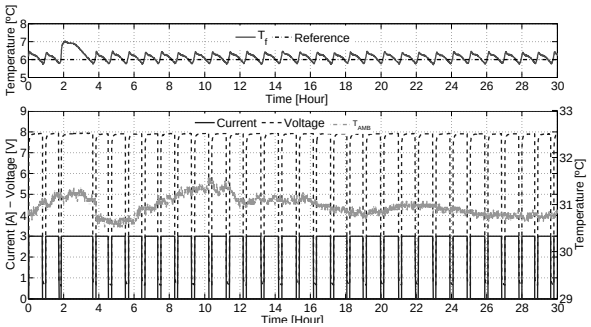

Fig. 16. Electrical energy consumption at 6^oC: thermostat.

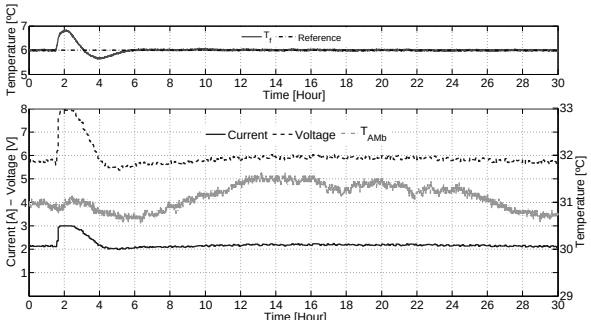

Fig. 17. Electrical energy consumption at 6^oC: MBPC.

TABLE III
ENERGY CONSUMPTION×ENERGY-SAVING.

	Energy Consumption [KWh/day]		
Temp [^{o}C]	Thermostat	MBPC	Energy-Save [%]
6	0.46	0.30	34.22
10	0.35	0.15	55.82

The MBPC system provides temperature control enabling requirements for energy consumption as ENERGYSTAR criterion, consuming 0.15KWh/day at 10^oC temperature regulation. The goal is not achieved for thermostat mode that requires 0.35KWh/day to regulation. In addition to achieving the requirements for certification, the MBPC allows a saving of 55.82% in electricity consumption over thermostat.

The MBPC allows saving 34.22% in energy consumption compared bistable control at 6^oC. It is the minimum saving offered by this new control strategy consuming 0.30kWh/day compared to 0.46KWh/day consumed by the bistable control.

The 0.30KWh/day consumption at 6^oC minimum set-point on MBPC mode is less than the 0.35KWh/day required for thermostat mode operate at 10^oC. The comparison ensure that MBPC technique allows full range operating energy savings.

VII. CONCLUSION

The thermoelectric cooling system was modeled around ANSI18 standard temperature specification. The phenomenological model was used to define the search space regressors vector for discrete model obtained through system identification technique.

The bistable controlled room temperature dynamic was noted in residue auto-correlation, since this is not explained by first order model considering the environment influence as model disturbance.

The MBPC tuning enables the system achieving equivalent performance to thermostat control and ANSI18 operational limits and performance requirements.

The control design proposed ensures disturbance rejection as room temperature variations and room temperature water replacement when its reservoir was drained. The methodology ensures energy-saving regulation throughout the operating range 6-10^oC.

The MBPC design enables achieving requirements for ENERGYSTAR Certified not feasible to bistable control project. The results encourage the hardware implementation for embedded control system.

REFERENCES

[1] S. B. Riffat and M. Xiaoli. Thermoelectrics: a review of present and potential applications. *Applied Thermal Engineering*, 23, 2003.

[2] Wilfred R. Schultz, Troy, and Mich. *Combined Hot and Cold Fluid Dispensing Apparatus*. U.S. patent 2912142. Sep. 10, 1959.

[3] G. Min and D.M. Rowe. Experimental evaluation of prototype thermoelectric domestic-refrigerators. *Applied Energy*, 83(2):133 – 152, 2006.

[4] M. Hodes. On one-dimensional analysis of thermoelectric modules (tems). *Components and Packaging Technologies, IEEE Transactions on*, 28(2):218–229, June 2005.

[5] D. Astrain and J. G.Vian. Computational model for refrigerators based on Peltier effect application. *Applied Thermal Engineering*, 25(17-18):3149 – 3162, 2005.

[6] ASHRAE. *Standard ANSI18: Methods of Testing for Rating Drinking-Water Coolers with Self-Contained Mechanical Refrigeration*. American Society of Heating, Refrigerating, and Air-Conditioning Engineers, United States, 2008.

[7] US-DOE. *ENERGY STAR® Program Requirements: Product Specification for Water Coolers*. US Environmental Protection Agency and US Department of Energy, United States, 2010.

[8] B. J. Huang and C.L. Duang. System dynamic model and temperature control of a thermoelectric cooler. *International Journal of Refrigeration*, 23:197–207, 2000.

[9] F.P. Incropera. *Fundamentals of heat and mass transfer*. Number v. 1 in Fundamentals of Heat and Mass Transfer. John Wiley, 2007.

[10] L. Ljung. *System Identification: Theory for the User*. Pearson Education, 1998.

[11] K.J. Åström and B. Wittenmark. *Computer-controlled systems: theory and design*. Prentice Hall information and system sciences series. Prentice Hall, 1997.

[12] C. Camacho, E. F. e Bordons. *Model Predictive Control*. Springer-Verlag, 2 edition, 2004.

[13] T.T.C. Tsang and D.W. Clarke. Generalised predictive control with input constraints. *Control Theory and Applications, IEE Proceedings D*, 135(6):451 – 460, nov 1988.

[14] D. W. Clarke, C. Mohtadi, and P. S. Tuffs. Generalized predictive control. part i the basic algorithm and part ii extensions and interpretations. 23(2):137 – 148, 1987.

[15] Philip Ball. Water - an enduring mystery. *Nature*, 452:291–292, 2008.